DALTON

Experimental and theoretical comparison between $M(cp)Cl_3L_n$ systems of Nb^{IV} and Mo^{IV} (cp = η-C_5H_5)†

D. Webster Keogh[a] **and Rinaldo Poli***‡[b]

[a] *Department of Chemistry and Biochemistry, University of Maryland, College Park, Maryland 20742, USA*
[b] *Laboratoire de Synthèse et d'Electrosynthèse Organométallique, Université de Bourgogne, Faculté des Sciences 'Gabriel', 6 Boulevard Gabriel, 21100 Dijon, France*

The controlled sodium reduction of $Nb(cp)Cl_4L$ (cp = η-C_5H_5; L = PMe_3, PMe_2Ph or $PMePh_2$) or $Nb(\eta$-$C_5Me_5)Cl_4$ in the presence of PMe_3 afforded the mononuclear 15-electron complexes $Nb(cp)Cl_3L$ and $Nb(\eta$-$C_5Me_5)Cl_3(PMe_3)$, respectively. Reduction of $Nb(cp)Cl_4$ in the presence of an excess of L for PMe_2Ph and $PMePh_2$ afforded solids that contain mainly the 17-electron $Nb(cp)Cl_3L_2$ species but are contaminated by the mono-L derivatives. A UV/VIS investigation of the solution equilibrium between $Nb(cp)Cl_3(PMe_2Ph)_2$ and $Nb(cp)Cl_3(PMe_2Ph)$ plus free PMe_2Ph afforded an enthalpy of 19.0 ± 1.6 kcal mol^{-1} and an entropy of 45 ± 5 cal K^{-1} mol^{-1} for the ligand dissociation process. A comparative study of the equilibrium between $Mo(cp)Cl_3(PMe_2Ph)_2$ and $Mo(cp)Cl_3(PMe_2Ph)$ plus free PMe_2Ph cannot be carried out because the equilibration is too slow at room temperature and because of thermal decomposition with ring loss at high temperature. Theoretical calculations at the second-order Møller-Plesset perturbation (MP2) level on the $M(cp)Cl_3(PH_3)_n$ (M = Nb or Mo, n = 1 or 2) model systems afforded geometries in good agreement with experimental examples. The calculated PH_3 dissociation energy for M = Nb of 21.3 kcal mol^{-1} is in good agreement with experiment. For M = Mo, the more saturated complex is stabilized by 32.8 kcal mol^{-1} relative to the excited $^1A'$ state and by 23.5 kcal mol^{-1} relative to the ground $^3A''$ state. Therefore, the regain of pairing energy upon PH_3 dissociation from $Mo(cp)Cl_3(PH_3)_2$ provides a calculated stabilization for the 16-electron monophosphine complex of 9.3 kcal mol^{-1}. The observed variations of bonding parameters upon metal change from Nb to Mo and a natural population analysis suggest that the main reason for a greater Mo–PH_3 bonding interaction is the greater extent of both M–P σ bonding and π back bonding for the d^2 metal relative to the d^1 metal.

We have been actively investigating the general area of intermediate-valent organometallic compounds that are characterized by an open-shell configuration and one or more unpaired electrons.[1] These compounds can be considered as bridging the gap between the two classical areas of co-ordination chemistry: Werner-type complexes on one side and low-valent organometallic complexes on the other.[2] The former complexes are characterized by prevalently ionic interactions, large pairing energies, open-shell configurations and the choice among different spin states, whereas the latter complexes are characterized by prevalently covalent interactions, small pairing energies, a closed-shell (18-electron) configuration, and a diamagnetic (S = 0) ground state. General principles from both the above-mentioned traditional areas of co-ordination chemistry must be used to rationalize the chemical behavior of the open-shell, intermediate-valent organometallic compounds.[2] Materials that belong to this class are interesting not only from the fundamental points of view of their electronic structure and bonding, but also for their potential applications in catalysis and materials chemistry.

We are particularly interested in quantifying the effect of a spin-state change on the energetics of a ligand association/dissociation reaction. For instance, if a ligand is dissociated from a diamagnetic 18-electron system the resulting 16-electron fragment may adopt either a spin-singlet or -triplet configuration. Taking the monoelectronic molecular orbital (MO) approach, we can view this process as transforming one M–L bonding orbital into a metal-based non-bonding orbital, which will be placed in the frontier region of the 16-electron M fragment (see Scheme 1). If the orbital splitting Δ is smaller than

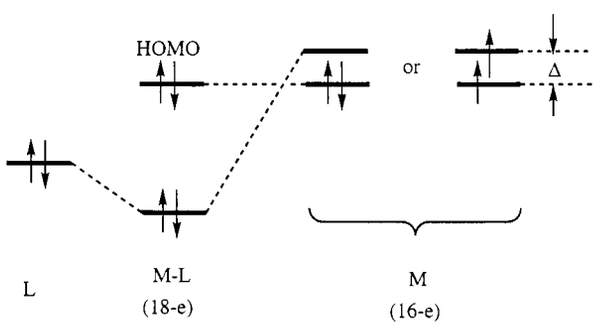

Scheme 1 HOMO = Highest occupied molecular orbital

the pairing energy, the M fragment will have a triplet ground state and the change of spin will contribute to lower the energetic demand of the ligand dissociation process and weaken the M–L bond. The first attribution of a weak bond dissociation enthalpy to a spin state change was probably that of the V–CO bond in $V(cp)_2I(CO)$ [13.1(10) kcal mol^{-1} (cp = η-C_5H_5); cal = 4.183 J] by Calderazzo *et al.*[3] The weaker M–CO bond in $M(cp)_2(CO)$ for M = Cr relative to Mo was also interpreted as the result of a change in the electron pairing energy.[4] Surprisingly, however, no general appreciation of this phenomenon has taken place until recently.

A recent example from our work is the dissociation of N_2 from $Mo(\eta$-$C_5Me_5)Cl(PMe_3)_2(N_2)$ to afford the paramagnetic (S = 1) $Mo(\eta$-$C_5Me_5)Cl(PMe_3)_2$ complex, the energy of the process being −22 ± 2 kcal mol^{-1} from equilibrium data.[5] Theoretical calculations on the $Mo(cp)Cl(PH_3)_2(N_2)$ model with geometry optimizations at the SCF–MP2 (self consistent field–second-order Møller-Plesset perturbation) level yielded a stabilization of 38.8 kcal mol^{-1} with respect to $Mo(cp)Cl(PH_3)_2$ ($^1A'$

† Dedicated to the memory of Sir Geoffrey Wilkinson.

‡ E-Mail: poli@u-bourgogne.fr

excited state) + N_2 and of 27.9 kcal mol^{-1} with respect to the corresponding $^3A''$ ground state. Therefore, breaking the Mo–N_2 bond is facilitated by the spin state change in the 16-electron system, which is worth 10.9 kcal mol^{-1}.[5] Singlet–triplet gaps in 16-electron complexes, even when the complexes can be isolated in a pure state, cannot be easily determined experimentally.

Another example from our recent work is represented by the molybdenum(IV) system Mo(cp)Cl_3L_n. For L = PMe_3 and PMe_2Ph, both diamagnetic, 18-electron (n = 2) compounds and spin-triplet 16-electron (n = 1) compounds have been observed in solution or isolated in the solid state. For L = $PMePh_2$, on the other hand, only the paramagnetic unsaturated material could be generated.[6,7] We therefore considered the possibility of comparing theory and experiment for this phosphine dissociation process. In addition, we decided to carry out the same studies on the isostructural d^1 niobium(IV) systems, Nb(cp)Cl_3L_n. The reason for this choice is that no spin-state change can occur in this case upon phosphine dissociation to the less saturated (n = 1) system. Thus, under the assumption that the bond strength would not be highly dependent on the metal nature, the determined value of the Nb^{IV}–L dissociation energy could be taken as a calibration point for the Mo^{IV}–L dissociation energy along the spin singlet surface. Both 17-electron Nb(cp)-Cl_3L_2 complexes [*e.g.* with L_2 = $Ph_2PCH_2CH_2PPh_2$ (dppe) or $Me_2PCH_2CH_2PMe_2$ (dmpe)][8,9] and 15-electron Nb(cp)Cl_3L complexes (*e.g.* with L = PMe_2Ph or $PMePh_2$)[10] have been previously described. In addition, we have recently reported the preparation of Nb(cp)$Cl_3(PMe_3)_2$ and obtained evidence for the existence of the corresponding 17-electron bis(PMe_2Ph) complex.[11] An equilibrium study on the M(cp)$Cl_3(PMe_2Ph)$ + PMe_2Ph process for both M = Nb and Mo appeared therefore feasible. All these studies, however, have revealed a more complex situation than expected, as will be shown in this contribution, which leads to new considerations on the nature of the M–PR_3 bonds for these early transition-metal systems.

Experimental

General

All operations were carried out under an atmosphere of argon. Solvents were dehydrated by conventional methods and distilled directly from the dehydrating agent prior to use [tetrahydrofuran (thf) and Et_2O from sodium–benzophenone, heptane and toluene from Na, and CH_2Cl_2 from P_2O_5]. The NMR spectra were recorded on Bruker WP200 and AF200 spectrometers; the peak positions are reported with positive shifts downfield of $SiMe_4$ as calculated from the residual solvent peaks (^1H) or downfield of external 85% H_3PO_4 (^{31}P). For each ^{31}P NMR spectrum a sealed capillary containing H_3PO_4 was immersed in the same NMR solvent used for the measurement and this was used as the external reference. The EPR spectra were recorded on a Bruker ER200 spectrometer equipped with an X-band microwave generator. The elemental analyses were by M-H-W Laboratories, Phoenix, Arizona or Galbraith Laboratories, Inc., Knoxville, TN. The compounds Nb(cp)Cl_4,[12] Nb(cp)-$Cl_4(PMe_3)$,[11] Nb(cp)$Cl_4(PMe_2Ph)$[11] and Nb(η-C_5Me_5)Cl_4[13] were prepared by literature methods; PMe_3 (Aldrich), PMe_2Ph (Aldrich) and $PMePh_2$ (Strem) were used as received without further purification.

Preparations

Nb(cp)$Cl_3(PMe_3)$ 1. The compound Nb(cp)$Cl_4(PMe_3)$ (0.225 g, 0.661 mmol) was added to a Schlenk tube containing thf (5 cm^3) and amalgamated Na (0.017 g, 0.739 mmol in 2 g Hg). The original red-orange solution turned purple after stirring overnight at room temperature. The solution was filtered through Celite and concentrated to *ca.* 1/3 the original volume by evaporation under reduced pressure. EPR [thf, room temperature (r.t.)]: broad decet of doublets, g = 1.986, a_{Nb} = 120.2 G, a_P = 22.0 G (G = 10^{-4} T); no signs of contamination with other materials [notably Nb(cp)$Cl_4(PMe_3)_2$, see below].

Nb(cp)$Cl_3(PMe_2Ph)$ 2. The compound Nb(cp)$Cl_4(PMe_2Ph)$ (0.150 g, 0.342 mmol) was added to thf (5 cm^3) and amalgamated Na (0.010 g, 0.435 mmol in 1.5 g Hg). The original red-orange solution turned purple after stirring overnight at room temperature. The solution was filtered through Celite and concentrated to *ca.* 1/3 the original volume by evaporation under reduced pressure. The addition of heptane (15 cm^3) precipitated a purple solid, which was washed with heptane (2 × 5 cm^3) and dried under vacuum. Yield: 0.091 g, 93% (Found: C, 36.39; H, 4.08. Calc. for $C_{13}H_{16}Cl_3NbP$: C, 36.91; H, 4.13%). EPR (thf, r.t.): decet of doublets, g = 2.013, a_{Nb} = 123.0 G, a_P = 26.0 G. UV/VIS (thf, r.t.): A_{max} = 500 nm (ε = 102 M^{-1} cm^{-1}).

Nb(cp)$Cl_3(PMePh_2)$ 3. The compound Nb(cp)Cl_4 (0.490 g, 1.63 mmol) was added to a thf solution (20 cm^3) of $PMePh_2$ (0.303 cm^3, 1.63 mmol) containing sodium sand (0.038 g, 1.65 mmol) and naphthalene, giving a red-orange solution. The solution became purple-brown after 30 min. After stirring overnight at room temperature, a purple precipitate in a purple thf solution was present. The solvent was removed under reduced pressure. The residue was extracted with CH_2Cl_2 (10, 5, 5 cm^3) and the extracts were filtered through Celite, until the washings were colorless. The CH_2Cl_2 solution was concentrated to approximately 5 cm^3 and heptane (10 cm^3) was added to precipitate a purple solid, which was dried under vacuum. Yield: 0.451 g, 60% (Found: C, 46.39; H, 4.03. Calc. for $C_{18}H_{18}Cl_3NbP$: C, 46.50; H, 3.64%). EPR (thf, r.t.): decet of broad singlets, g = 1.989, a_{Nb} = 124.3 G.

Nb(cp)$Cl_3(PMe_3)_2$ 4, in admixture with compound 1. The compound Nb(cp)Cl_4 (0.564 g, 1.88 mmol) was added to a toluene solution (40 cm^3) of PMe_3 (0.400 cm^3, 3.86 mmol) over Na/Hg (0.046 g, 2.00 mmol in 6 g of Hg) giving a red-orange solution. After 30 min of stirring at room temperature the solution became green. After 12 h of stirring at room temperature the toluene was removed under reduced pressure and the residue was extracted with CH_2Cl_2 until the washings were colorless (10, 5, 5 cm^3). After filtration through Celite the green solution was concentrated to *ca.* 1/3 of the original volume by evaporation under reduced pressure. Heptane (10 cm^3) was added to precipitate a green solid, which was then washed with heptane (2 × 5 cm^3) and dried under vacuum. Yield: 0.588 g, 75%. The compound can be recrystallized by diffusion of a heptane layer into a toluene solution (Found: C, 30.81; H, 5.75. Calc. for $C_{11}H_{23}Cl_3NbP_2$: C, 31.72; H, 5.58%). The low C, H analyses are attributed to the presence of **1**, which is confirmed by EPR spectroscopy. EPR (thf, r.t.): decet of triplets, g = 1.988, a_{Nb} = 121.0 G, a_P = 17.8 G.

Nb(cp)$Cl_3(PMe_2Ph)_2$ 5, in admixture with compound 2. The compound Nb(cp)Cl_4 (0.769 g, 2.56 mmol) was added to a toluene solution (50 cm^3) of PMe_2Ph (0.730 cm^3, 5.13 mmol) containing Na/Hg (0.126 g, 5.48 mmol in 11 g of Hg) giving a red-orange solution. After 30 min of stirring the solution became green. After stirring overnight at room temperature the toluene was only lightly colored and was removed under reduced pressure. The residue was extracted with CH_2Cl_2 (2 × 15 cm^3). After filtration through Celite the green solution was concentrated to *ca.* 5 cm^3 by evaporation under reduced pressure. Heptane (10 cm^3) was added producing a green oil. The oil was dried under reduced pressure, washed with heptane (2 × 5 cm^3) and dried under vacuum again. Yield: 0.946 g, 68% (Found: C, 42.97; H, 5.16. Calc. for $C_{21}H_{27}Cl_3NbP_2$: C, 44.17; H, 5.27%). The low C, H analyses are attributed to the presence of **2**, which is confirmed by EPR spectroscopy. EPR (thf, r.t.): decet of triplets,

$g = 1.997$, $a_{Nb} = 120.3$ G, $a_P = 24.1$ G. UV/VIS (thf, r.t.): $A_{max} = 396$ nm ($\varepsilon = 279$ M^{-1} cm^{-1}).

Nb(η-C_5Me_5)Cl_3(PMe_3) 6. The compound Nb(η-C_5Me_5)Cl_4 (0.254 g, 0.687 mmol) was added to a thf solution (15 cm^3) of PMe_3 containing sodium sand (0.018 g, 0.783 mmol) and naphthalene (0.01 g), giving a purple-red solution. The mixture was allowed to stir overnight leading to a dark purple solution. The solvent was removed under reduced pressure and the residue was extracted with CH_2Cl_2 (3 × 10 cm^3). After filtration through Celite, the combined extracts were concentrated to approximately 5 cm^3 by evaporation under reduced pressure and a purple solid was precipitated by adding heptane (20 cm^3). The solid was filtered off, washed with heptane (2 × 5 cm^3) and dried under vacuum. Yield: 0.237 g, 84%. EPR (thf, r.t.): decet of doublets, $g = 2.007$, $a_{Nb} = 128.6$ G, $a_P = 27.1$ G. Although the EPR spectrum did not show signs of contamination with other materials, satisfactory analytical data could not be obtained for this compound.

[Mo(cp)Cl_2(PMe_2Ph)$_2$][PF_6] 9. The compound Mo(cp)Cl_2-(PMe_2Ph)$_2$ was prepared as previously described[14] from Mo(cp)Cl_2 (0.331 g, 1.43 mmol) and PMe_2Ph (0.406 cm^3, 2.86 mmol) in CH_2Cl_2 (25 cm^3). After stirring for 3 h the clear red-brown solution was filtered. The compound [Fe(cp)$_2$][PF_6] (0.475 g, 1.44 mmol) was added giving rise to an immediate change to dark red-orange. After 1 h of stirring the solution was concentrated under reduced pressure to *ca.* 5 cm^3. Heptane (20 cm^3) was added to precipitate a red solid, which was subsequently filtered off, washed with heptane (3 × 5 cm^3) and dried. Yield: 0.814 g, 87% (Found: C, 38.66; H, 4.14. Calc. for $C_{21}H_{27}Cl_2F_6MoP_3$: C, 38.61; H, 4.17%). ^{1}H NMR ($CDCl_3$, r.t.): δ 73.5 (br s, $w_{\frac{1}{2}} = 775$, 5 H, C_5H_5), 15.0 (br s, $w_{\frac{1}{2}} = 91$, 4 H, *o*-H of PMe_2*Ph*), 9.11 (br s, $w_{\frac{1}{2}} = 30$, 4 H, *m*-H of PMe_2*Ph*), 6.72 (s, 2 H, *p*-H of PMe_2*Ph*) and −9.62 (br s, $w_{\frac{1}{2}} = 183$ Hz, 12 Hz, P*Me*$_2$Ph).

General procedures for the equilibrium studies by UV/VIS spectroscopy

A stock solution (6.5×10^{-3} M) was prepared by dissolving compound **2** (0.052 g) in thf (20 cm^3). For the evaluation of K_{eq} of equilibrium (1) at 25 °C, an aliquot (3 cm^3) was taken and the initial UV/VIS spectrum taken. Varying amounts of PMe_2Ph were subsequently added and the visible absorbance at 500 nm monitored. The data were fitted by equation (2), which was derived using Beer's law and equation (1), where A is the absorbance, C_0 and C_p are given in equations (3) and (4) and ε_A,

$$Nb(cp)Cl_3(PMe_2Ph) + PMe_2Ph \rightleftharpoons Nb(cp)Cl_3(PMe_2Ph)_2 \quad (1)$$

$$A = (\varepsilon_B - \varepsilon_A) \times \left[\frac{(C_0 + C_p + K_{eq}^{-1}) - \sqrt{(C_0 + C_p + K_{eq}^{-1})^2 - 4C_0C_p}}{2}\right] + C_0\varepsilon_A \quad (2)$$

$$C_0 = [Nb(cp)Cl_3(PMe_2Ph)]_{initial} = [Nb(cp)Cl_3(PMe_2Ph)] + [Nb(cp)Cl_3(PMe_2Ph)_2] \quad (3)$$

$$C_p = [PMe_2Ph]_{added} = [PMe_2Ph] + [Nb(cp)Cl_3(PMe_2Ph)_2] \quad (4)$$

ε_B are the molar absorption coefficients of species **5** and **2**, respectively. The best curve (see Fig. 1) was determined by an iterative process (quasi-Newtonian method) with the program CURVE FIT[15] using A, C_0 and C_p as data and K_{eq}, ε_A and ε_B as parameters.

A variable temperature ($T = 32.0$ to 59.8 °C) study of K_{eq} was subsequently carried out at a single C_p (*ca.* 1 equivalent relative to C_0), using 3 cm^3 (0.019 mmol) of the same stock solution as above and 2.5 μl of PMe_2Ph (0.018 mmol). The solution was thermostatted in the UV/VIS block. Qualitatively, as the temperature was raised an increase of **[2]** and consequently a decrease in **[5]** were observed. The determination of **[2]** was carried out by monitoring the absorbance at 500 nm under the assumption that ε_A and ε_B are temperature independent. This was confirmed for ε_B by monitoring the UV/VIS spectrum of a thf solution of **2** between 0 and 45 °C. The values of K_{eq} at each temperature are given in Table 1.

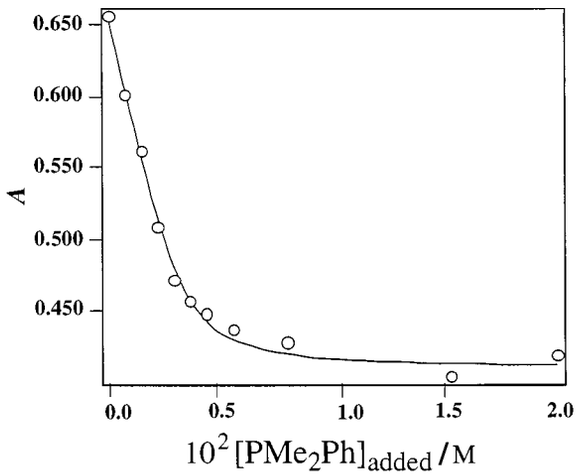

Fig. 1 Plot of $A_{500\,nm}$ *versus* C_p for equilibrium (1) at 20 °C

Table 1 Experimental data for the equilibrium (1)

T/K	10^{-3} K_{eq}/M^{-1}
298(1)	10.7(14)
314.65(5)	2.75(16)
318.65(5)	2.11(12)
319.45(5)	1.85(12)
323.25(5)	1.23(8)
328.95(5)	0.68(4)
332.95(5)	0.37(2)

Theoretical calculations

Geometry optimizations at the SCF–MP2 level were carried out with the GAUSSIAN 94 package.[16] The LANL2DZ basis set without polarization functions includes both Dunning and Hay's D95 sets for H and C and relativistic electron core potential (ECP) sets of Hay and Wadt[17–19] for the heavier atoms. Electrons outside of the core were all those of the H and C atoms, the 4s, 4p, 4d and 5s electrons in the Mo and Nb atoms and the 3s and 3p electrons in Cl and P atoms. The input coordinates for M(cp)Cl_3(PH_3) and M(cp)Cl_3(PH_3)$_2$ (M = Nb or Mo) were adapted from coordinates published for Mo(η-C_5Me_5)Cl_3(PMe_3)[7] and Mo(cp)Cl_3(PMe_2Ph)$_2$,[7] respectively. A C_s symmetry was imposed for all systems. The mean value of the spin of the first-order electronic wavefunction, which is not an exact eigenstate of S^2 for unrestricted Hartree–Fock (HF) calculations on open-shell systems, was considered suitable unambiguously to identify the spin state. Spin contamination was carefully monitored and the energies shown in the Results section correspond to unrestricted MP2 (UMP2) calculations. The value of $\langle S^2 \rangle$ for the UHF calculations at convergence was 0.7820 for Nb(cp)Cl_3(PH_3), 0.7920 for Nb(cp)Cl_3(PH_3)$_2$ and 2.1565 for ^{3}A″ Mo(cp)Cl_3(PH_3), indicating minor spin contamination.

Results

Synthesis and characterization of the niobium(IV) compounds

We have recently shown[11] that niobium(IV) half-sandwich complexes of the type Nb(cp)Cl_3L_n ($n = 2$, L = PMe_3 or PMe_2Ph;

$n = 1$, L = PMe_2Ph) are obtained as by-products *via* reduction by an excess of phosphine during the synthesis of the monodentate phosphine adducts of $Nb(cp)Cl_4$. In the present study we have optimized the synthetic procedure for the production of either 15- or 17-electron complexes $Nb(cp)Cl_3L_n$ ($n = 1$ or 2). This involves reduction of $(cp)Nb^V$ complexes with Na in the presence of the appropriate amount of phosphine. The 15-electron complexes $Nb(cp)Cl_3L$ (L = PMe_2Ph or $PMePh_2$) have been previously described, but the synthesis did not follow a logical approach and the final products were reported as dichloromethane solvates.[10] The procedure reported here provides materials of higher purity. All the d^1 niobium(IV) complexes are EPR active and show in all cases the expected couplings to the ^{31}P ($I = \frac{1}{2}$, 100%) and Nb ($I = \frac{9}{2}$, 100%) nuclei.

For the PMe_3 system, the use of 1 equivalent of the ligand allows the formation of the purple-brown, 15-electron complex **1**, see equation (5). The use of 2 equivalents of PMe_3, on the

$$Nb(cp)Cl_4L + Na \xrightarrow[L = PMe_3,\ PMe_2Ph,\ PMePh_2]{thf} Nb(cp)Cl_3L + NaCl \quad (5)$$

other hand, led to the isolation of the green 17-electron system, **4** [equation (6)]. The low C, H analyses for **4** are rationalized

$$Nb(cp)Cl_4 + 2L + Na \xrightarrow[L = PMe_3,\ PMe_2Ph]{thf} Nb(cp)Cl_3L_2 + NaCl \quad (6)$$

with the presence of minor amounts of **1**, thus indicating a phosphine dissociation equilibrium. The presence of **1** as an impurity in **4** is also evident from the EPR spectrum. A similar 15-electron product **6** was also obtained when the ring system was changed from cp to the more sterically encumbered C_5Me_5 ligand [equation (7)]. Excess amounts of PMe_3 did not lead to

$$Nb(\eta\text{-}C_5Me_5)Cl_4 + PMe_3 + Na \xrightarrow{thf} Nb(\eta\text{-}C_5Me_5)Cl_3(PMe_3) + NaCl \quad (7)$$

the formation of any 17-electron product in this case. This behavior parallels that of Mo^{IV}: both $Mo(cp)Cl_3(PMe_3)_n$ ($n = 1$ or 2) have been observed,[6] while the C_5Me_5 system is only capable of affording the 16-electron $Mo(\eta\text{-}C_5Me_5)Cl_3(PMe_3)$.[7] It should be pointed out that the best results for the formation of **1** were obtained by using the preformed complex $Nb(cp)Cl_4(PMe_3)$,[11] rather than a 1:1 mixture of $Nb(cp)Cl_4$ and PMe_3. This is because PMe_3 also undergoes a reductive side reaction with $Nb(cp)Cl_4$, as previously described in detail.[11] The synthesis of **4**, on the other hand, is not sensitive to the P:Nb stoichiometry and $Nb(cp)Cl_4$ can be conveniently used as a starting material.

The cp/PMe_2Ph system behaves in a manner similar to the cp/PMe_3 system: the use of 1 equivalent of the phosphine leads to a purple 15-electron product, **2**, while 2 equivalents or more lead to the green bis(PMe_2Ph) product, **5**. Again, EPR spectroscopy and analytical (C, H) data indicate that **5** is contaminated with compound **2**. The equilibrium between **2** and **5** was subsequently examined in more detail (see below). In the case of the $PMePh_2$ system only a purple 15-electron complex, **3**, was obtained [equation (5)]. Addition of an excess of $PMePh_2$ to complex **3** had no effect on the EPR and UV/VIS spectroscopic properties. Once again, this behavior parallels that observed previously for the corresponding molybdenum(IV) systems.[7]

The EPR spectra of the 17-electron complexes **4** and **5** consist of decets of triplets and are in excellent agreement with the spectrum of the previously described $Nb(cp)Cl_3(dmpe)$, $g = 1.971$, $a_{Nb} = 135$ G, $a_P = 14.3$ G.[9] For the 15-electron complexes, **1**–**3** and **6**, EPR patterns consisting of decets of doublets are expected and indeed observed for **1**, **2** and **6**. These are analogous to the spectrum previously reported for **2**·CH_2Cl_2.[10] For compound **3** the phosphorus coupling is not discerned resulting in a decet of broad resonances which did not sharpen upon cooling to −60 °C, in agreement with the literature.[10] The EPR spectra of the 15-electron compounds are identical in thf and in CH_2Cl_2, suggesting that co-ordination of thf to afford hypothetical 17-electron $Nb(cp)Cl_3L(thf)$ does not occur.

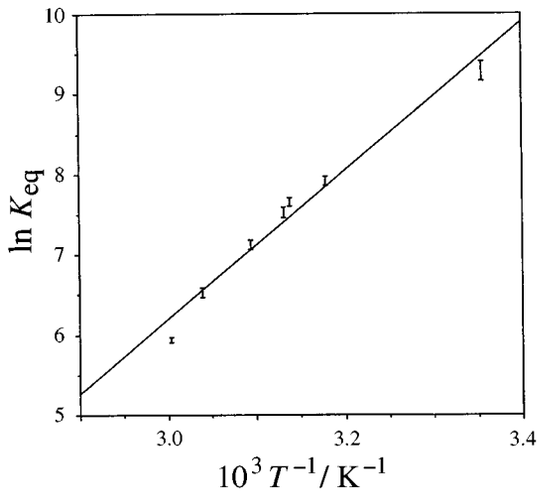

Fig. 2 Plot of ln K_{eq} *versus* T^{-1} for equilibrium (1)

Study of equilibrium 1

As stated above, attempts at generating compound **5** by using stoichiometric amounts of PMe_2Ph resulted in the isolation of a mixture of **5** and **2**, according to equilibrium (1). Experiments to determine the value for the equilibrium constant as well as the thermodynamic parameters were performed. Since there is a drastic difference in the colors of **2** (red-purple $\varepsilon_{500\ nm} = 102$ M^{-1} cm^{-1}) and **5** (green, $\varepsilon_{500\ nm} = 65$ M^{-1} cm^{-1} for a solution obtained from **2** and 5 equivalents of PMe_2Ph), the technique chosen to study the equilibrium was visible spectroscopy. The initial experiment was carried out at 20 °C by monitoring the absorbance at 500 nm upon addition of variable amounts of PMe_2Ph to **2**. An isosbestic point was observed at 420 nm throughout the addition of 1.2 mol of PMe_2Ph per mol of **4**. The departure from this isosbestic behavior at greater concentrations of PMe_2Ph is tentatively attributed to a reduction process by excess of phosphine ligand which takes the niobium(IV) complex to a niobium(III) species. This behavior would parallel the demonstrated reduction of $(cp)Nb^V$ to niobium(IV) species by excess of phosphine.[11] Since the effect of this process is limited to the end-points of the experiment, no significant error is expected for the calculation of K_{eq}. The large value of K_{eq} (Table 1) indicates that the equilibrium is well shifted to the right. The determination of the equilibrium position at higher temperature was determined at a single PMe_2Ph:Nb ratio by mixing the appropriate amounts of **2** and PMe_2Ph. The plot of ln K_{eq} *versus* T^{-1} is shown in Fig. 2. Analysis of the slope and intercept of this plot resulted in the determination of $\Delta H = -19.0 \pm 1.6$ kcal mol^{-1} and $\Delta S = -45 \pm 5$ cal K^{-1} mol^{-1} for equilibrium (1).

The UV/VIS absorption spectrum of compound **2** was found to be invariant in different solvents (CH_2Cl_2, thf and toluene) and the ε_{max} is small, in agreement with the attribution of this absorption to a d–d transition. If this absorption were due to a metal to ligand or ligand to metal charge-transfer transition a linear correlation between solvent polarity and λ_{max} would be expected.

Experimental investigations on the molybdenum(IV) system

A goal of this study (see Introduction) was the comparison of

equilibrium (1) with that of the corresponding molybdenum(IV) system, *i.e.* equilibrium (8). Both compounds $Mo(cp)Cl_3$-

$$Mo(cp)Cl_3(PMe_2Ph) + PMe_2Ph \rightleftharpoons Mo(cp)Cl_3(PMe_2Ph)_2 \quad (8)$$

(PMe_2Ph) **7** and $Mo(cp)Cl_3(PMe_2Ph)_2$ **8** have been previously obtained from the controlled addition of PMe_2Ph to $Mo(cp)Cl_3$.[7] However, **7** could not be isolated as a pure crystalline solid, whereas **8** was obtained in the form of single crystals which were structurally characterized by X-ray crystallography. A bulk synthesis of analytically pure **8**, however, was not available.[7] Repeated attempts to isolate pure crystalline **7** have failed, whereas the synthesis of **8** in bulk quantities always led to a material that was contaminated by small but significant amounts of **7**.

Since equilibrium (8) could not be investigated starting from either pure compound **7** and PMe_2Ph or from pure **8**, it was necessary to find alternative methods to generate solutions with known total analytical concentrations of Mo (*i.e.* [**7**] + [**8**]) and phosphine (*i.e.* [PMe_2Ph] + [**7**] + 2[**8**]). The fact that **7** is paramagnetic renders impossible the use of NMR integration against an inert standard for the quantification of mixtures of the two compounds. The possibility that was first considered was the *in situ* addition of controlled amounts of PMe_2Ph to $Mo(cp)Cl_3$. A ^{1}H NMR monitoring of the interaction, however, revealed the formation of minor amounts of by-products, among which the known[20] $MoCl_3(PMe_2Ph)_3$ was recognized. The extensive formation of $MoCl_3(PMe_3)_3$ from $Mo(cp)Cl_3$ and PMe_3 has been previously reported.[21] Although this side reaction apparently does not hamper the formation of the major products, *i.e.* compounds **7** and **8**,[7] this method cannot be used for the accurate determination of equilibrium (8).

Another possibility would consist in the use of a crystalline 16-electron compound of type $Mo(cp)Cl_3L$ which would undergo complete substitution of L upon addition of PMe_2Ph. Such a method would offer the additional advantage of generating free L at known concentrations as an internal standard for NMR integration. This strategy has been successfully employed by us for the generation, for kinetic purposes, of solutions of the molybdenum(III) complex $Mo(cp)Cl_2(PEt_3)_2$ from $Mo(cp)Cl_2(PPh_3)_2$ and PEt_3.[22] However, it is known that $Mo(cp)Cl_3$ does not form an adduct with thf[21,23] and we now find no interaction between $Mo(cp)Cl_3$ and PPh_3. The reaction of $Mo(cp)Cl_3$ with $PMePh_2$ affords crystalline $Mo(cp)Cl_3(PMePh_2)$,[7] but an investigation of the interaction of the latter compound with PMe_2Ph indicates that the ligand exchange is not complete. Therefore, this strategy is also unsuitable for the investigation of equilibrium (8).

A final attempted strategy consisted in the generation of $[Mo(cp)Cl_2(PMe_2Ph)_2]^+$ $\mathbf{9}^+$ by the known[14] one-electron oxidation process of the molybdenum(III) neutral precursor, followed by the addition of Cl^-. This method should lead to a solution of pure **8** at known concentration according to equation (9).

$$[Mo(cp)Cl_2(PMe_2Ph)_2]^+ + Cl^- \longrightarrow Mo(cp)Cl_3(PMe_2Ph)_2 \quad (9)$$

Complex $\mathbf{9}^+$ was readily obtained as the PF_6^- salt by oxidation of $Mo(cp)Cl_2(PMe_2Ph)_2$ with $[Fe(cp)_2][PF_6]$ and was characterized by C, H elemental analysis and ^{1}H NMR spectroscopy. The ^{1}H NMR spectrum indicates that the compound has a spin triplet ground state, as is well established for molybdenum(IV) systems of this stoichiometry.[6,7,24]

The administration of the stoichiometric amount of Cl^- to solutions of [**9**][PF_6] in $CDCl_3$ as solvent indeed leads to solutions of compound **8**. This reaction was carried out in the presence of a known amount of PPh_3 as an internal ^{31}P NMR standard. The subsequent NMR measurements indicate that **8** is indeed formed as expected. The ^{1}H NMR spectrum did not show any evidence for the presence of **7** and free PMe_2Ph. Small concentrations of these two compounds could be difficult to detect in the ^{1}H NMR spectrum because the resonances of **7** are broad and paramagnetically shifted, whereas those of free PMe_2Ph may be overshadowed by those of **8**. However, ^{31}P NMR spectroscopy reveals the presence of **8** and free PPh_3 and the absence of a resonance that could be attributed to free PMe_2Ph. However, we have previously observed and reported that solutions containing, among other by-products, compounds **7**, **8** and free PMe_2Ph are obtained from the direct interaction of PMe_2Ph and $Mo(cp)Cl_3$.[7] These solutions do not change the relative concentration of **7** and **8** over an extended period of time at room temperature. These observations collectively demonstrate that equilibrium (8) is slow at room temperature. To circumvent the kinetic problem, solutions obtained as described in reaction (9) were investigated at higher temperature (up to 80 °C). Prolonged heating at this temperature, however, induced decomposition with formation of $MoCl_3(PMe_2Ph)_3$. The conclusion of this experimental study is that equilibrium (8) is too slow to be investigated at temperatures at which the compounds do not thermally decompose. The study of an equilibrium between a 16-electron, spin triplet monophosphine and an 18-electron, spin singlet bis(phosphine) $(cp)Mo^{IV}$ derivative could only be investigated theoretically, as shown in the next section.

Theoretical calculations

The calculations consisted of unrestricted open-shell SCF followed by a second-order Møller-Plesset (MP2) geometry optimization (see Experimental section) on both sides of equations (10) and (11). This method has recently been applied to the

$$Nb(cp)Cl_3(PH_3) + PH_3 \rightleftharpoons Nb(cp)Cl_3(PH_3)_2 \quad (10)$$

$$Mo(cp)Cl_3(PH_3) + PH_3 \rightleftharpoons Mo(cp)Cl_3(PH_3)_2 \quad (11)$$

investigation of other equilibria involving a spin state change, *i.e.* $M(cp)X_2(PH_3) + PH_3 \rightleftharpoons M(cp)X_2(PH_3)_2$ (M = Cr or Mo, X = Cl or CH_3)[25,26] and $Mo(cp)Cl(PH_3)_2 + L \rightleftharpoons Mo(cp)Cl(PH_3)_2L$ (L = CO or N_2),[5] and its suitability to reproduce experimental geometries (distances within 0.1 Å, angles within 3°) and relative energies was demonstrated. Both niobium(IV) systems, $Nb(cp)Cl_3(PH_3)_n$ ($n = 1$ or 2), were calculated in the $S = \frac{1}{2}$ configurations. The 18-electron system $Mo(cp)Cl_3(PH_3)_2$ was calculated in the $S = 0$ configuration, whereas the 16-electron $Mo(cp)Cl_3(PH_3)$ system was calculated in both possible $S = 0$ and 1 configurations.

The optimized geometrical parameters are collected in Table 2 for the niobium(IV) system and in Table 3 for the molybdenum(IV) system, in comparison with those of related structurally characterized compounds. For the 17-electron niobium(IV) system the only crystallographically characterized complex is $Nb(cp)Cl_3(dppe)$,[27] which has a pseudo-octahedral geometry with the dppe ligand chelating an axial and an equatorial position (*i.e. mer-cis*). The geometry of $Nb(cp)Cl_3(PH_3)_2$, however, was optimized for the alternative *mer-trans* stereochemistry, because the $Nb(cp)Cl_3L_2$ (L = PMe_3 or PMe_2Ph) complexes reported here are more likely to adopt this structure, which is observed for the analogous molybdenum(IV) complex $Mo(cp)Cl_3(PMe_2Ph)_2$ and is further suggested by the equivalence of the P nuclei in the EPR spectra. As a result, a direct comparison between the calculated and experimental parameters for this system is not very meaningful, especially in terms of the bond angles. However, within these limitations, the calculated parameters compare relatively well with the experimental data. The largest deviation in the bond lengths is for the Nb–Cl bond (*ca.* 0.1 Å too long from the calculations).

For the 15-electron niobium(IV) system no crystallographically characterized complex is available. The optimized Nb–C

and Nb–Cl distances expectedly shorten on going from the 17-electron to the less saturated 15-electron niobium(IV) system (by *ca.* 0.1 Å for Nb–Cl, 0.04 Å for Nb–C), whereas the Nb–P distance correspondingly lengthens by 0.04 Å.

The optimized geometries for the molybdenum(IV) systems are also in good agreement with those experimentally determined (see Table 3). The largest deviation for the bond distances, as for the niobium(IV) systems discussed above, is a *ca.* 0.1 Å lengthening for the calculated Mo–Cl bond, both for 18- and 16-electron systems. The angular parameters are also in excellent agreement, especially considering that these are very sensitive to the nature of the ligands and to the electronic configuration for four-legged piano-stool structures.[28] The largest deviation in the CNT(centroid)–Mo–X angles is *ca.* 2.5° when X = P. As for the Nb^{IV} described above, a shortening of the Mo–Cl (by *ca.* 0.1 Å) and Mo–C (by *ca.* 0.03 Å) and a slight lengthening of the Mo–P bond (by 0.02 Å) is observed on going from the more saturated to the less saturated system (in the same $S = 0$ configuration). Within the 16-electron system, a change of spin state from singlet to triplet lengthens all bonds except the Mo–Cl bond that is *trans* to PH_3.

The electronic structure of the four-legged piano stool has been the subject of several theoretical analyses.[28–30] After formation of the metal–ligand bonds, the orbitals remaining available for occupation by the metal electrons are mainly composed of the metal d_{z^2} and d_{xy} orbitals. These have the proper symmetry to engage in M–Cl π*, M–P π and M–Cl δ interactions [see Scheme 2(*a*)]. For the pseudo-octahedral complexes of stoichiometry $M(cp)Cl_3L_2$, only the d_{xy} orbital remains available for the metal electrons, since the d_{z^2} orbital is engaged in the σ bonding with the new axial ligand [Scheme 2(*b*)]. This orbital is still available for π interactions with the Cl (only pseudo-equatorial, antibonding) and P (bonding) donors, as well as a δ interaction with the cp ligand. On the other hand, no π interaction is symmetry allowed between this orbital and the axial Cl ligand.

The energy picture for all systems of Nb^{IV} and Mo^{IV} is summarized in Fig. 3. The calculations for the niobium(IV) system showed the 17-electron complex to be the thermodynamically favored species with a Nb–P bond energy of 21.3 kcal mol^{-1}. The 16-electron molybdenum(IV) system has a calculated triplet

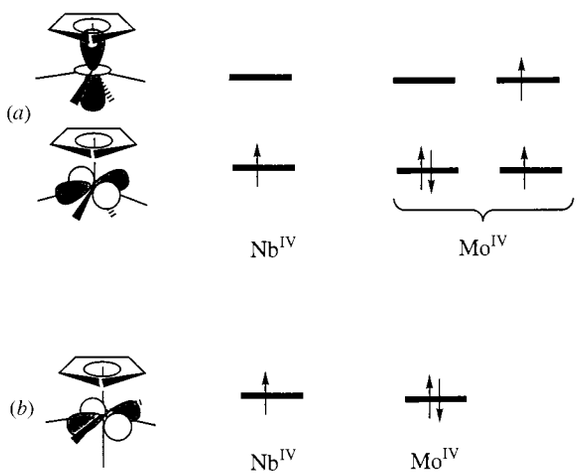

Scheme 2

Table 2 Selected geometrical parameters for 15- and 17-electron $Nb(cp)Cl_3L_n$ complexes ($n = 1$ or 2). The units are Å for bond lengths and degrees for bond angles

	Calculated		Experimental
	$Nb(cp)Cl_3(PH_3)$ ($^2A''$)	$Nb(cp)Cl_3(PH_3)_2$ ($^2A'$)	$Nb(cp)Cl_3$(dppe)[a] ($S = \frac{1}{2}$)
Nb–Cl[b]	2.465	2.583	—
Nb–Cl[c]	2.497	2.575	2.473(9)
Nb–P	2.720	2.679	2.678(1)[d]
Nb–C (average)	2.466	2.500	2.41(4)
Nb–CNT	2.133	2.174	2.099(5)
P–H (average)	1.4227	1.4233	
P–Nb–Cl[b]	142.72	73.36	—
P–Nb–Cl[c]	77.86	86.90	86(6)[d]
Cl[b]–Nb–Cl[c]	87.76	79.06	—
Cl[c]–Nb–Cl[c]	132.81	158.10	149.70(4)
P–Nb–P	—	146.72	—
CNT–Mo–Cl[b]	109.80	180.00	—
CNT–Mo–Cl[c]	112.84	100.95	105.2(8)
CNT–Mo–P	107.48	106.64	101.4(1)
E[e]/hartree	−301.0127	−309.1242	

[a] Data are taken from ref. 27. [b] Axial position for the 17-electron complex, *trans* to P for the 15-electron complex. [c] Equatorial positions for the 17-electron complex, *cis* to P for the 15-electron complex. [d] To the equatorial phosphorus atom. [e] The energy of PH_3 was calculated as −8.0776 hartree; 1 hartree (E_h) ≈ 4.36 × 10^{-18} J.

Table 3 Selected geometrical parameters for 16- and 18-electron $Mo(cp)Cl_3L_n$ complexes ($n = 1$ or 2). The units are Å for bond lengths and degrees for bond angles

	Experimental	Experimental	Calculated			Experimental
	$Mo(\eta\text{-}C_5Me_5)Cl_3(PMe_3)$[a] ($S = 1$)	$Mo(\eta\text{-}C_5Me_5)Cl_3(PMePh_2)$[a] ($S = 1$)	$Mo(cp)Cl_3(PH_3)$ ($^3A''$)	$Mo(cp)Cl_3(PH_3)$ ($^1A'$)	$Mo(cp)Cl_3(PH_3)_2$ ($^1A'$)	$Mo(cp)Cl_3(PMe_2Ph)_2$[a] ($S = 0$)
Mo–Cl[b]	2.420(3)	2.405(4)	2.439	2.472	2.575	2.461(1)
Mo–Cl[c]	2.399(3)	2.382(3)	2.493	2.466	2.595	2.527(1)
Mo–P	2.533(3)	2.578(3)	2.592	2.565	2.542	2.554(1)
Mo–cp (average)	2.36(1)	2.36(1)	2.413	2.346	2.375	2.309(4)
Mo–CNT	2.038(9)	2.03(1)	2.071	1.990	2.025	
P–H (average)			1.4203	1.4233	1.4240	
P–Mo–Cl[b]	131.1(1)	126.5(1)	131.93	143.64	72.93	75.6(1)
P–Mo–Cl[c]	77.4(1)	77.8(2)	76.29	79.79	86.43	87.1(1)
P–Mo–P	—	—	—	—	145.70	150.4(1)
Cl[b]–Mo–Cl[c]	83.5(1)	83.0(6)	86.23	85.33	77.76	78.0(1)
Cl[c]–Mo–Cl[c]	132.2(1)	137.6(1)	134.94	130.63	155.52	156.0(1)
CNT–Mo–Cl[b]	113.2(3)	112.7(3)	113.00	106.07	178.62	175.5
CNT–Mo–Cl[c]	114.8(10)	111.2(4)	111.92	114.59	102.25	102.0
CNT–Mo–P	115.8(3)	120.8(4)	115.08	110.29	107.11	104.6
E[d]/hartree			−312.1015	−312.0867	−320.2165	

[a] Data taken from ref. 7. [b] Axial position for the 18-electron complex, *trans* to P for the 16-electron complex. [c] Equatorial positions for the 18-electron complex, *cis* to P for the 16-electron complex. [d] The energy of PH_3 was calculated as −8.0776 hartree.

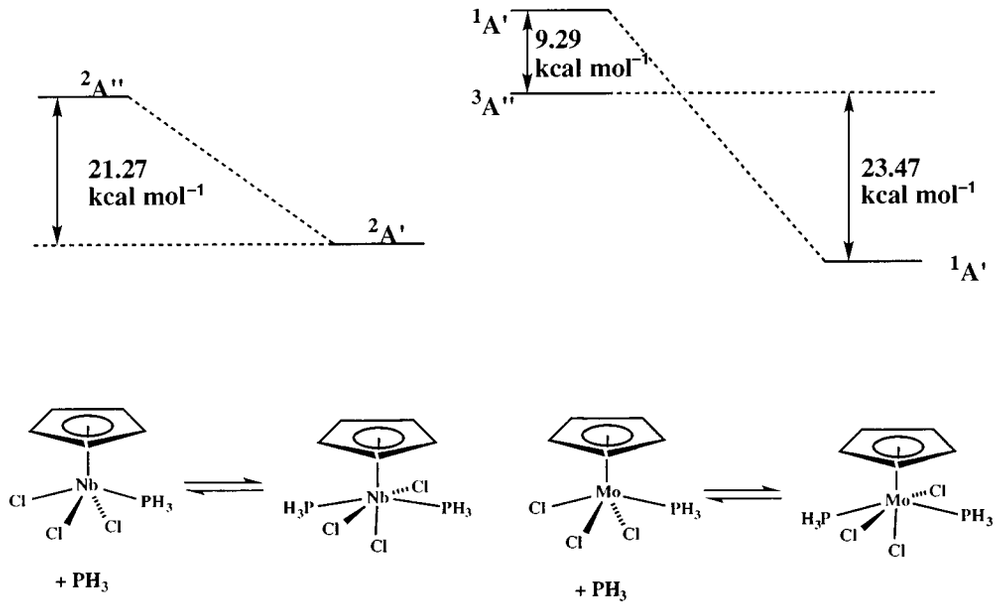

Fig. 3 Qualitative energy diagram for the MP2 theoretical calculations for the 15/17-electron $Nb(cp)Cl_3(PH_3)_n$ ($n = 1$ or 2) and the 16/18-electron $Mo(cp)Cl_3(PH_3)_n$ ($n = 1$ or 2) systems

ground state ($^3A''$), with an energy gap to the singlet excited state ($^1A'$) of 9.3 kcal mol^{-1}. The 18-electron molybdenum(IV) complex, however, is thermodynamically favored with respect to the PH_3 dissociation process, with a stabilization of 23.5 kcal mol^{-1} relative to the $^3A''$ state and 32.8 kcal mol^{-1} relative to the $^1A'$ state.

Discussion

The structures and phosphine dissociation equilibria of niobium(IV) complexes of type $Nb(cp)Cl_3L_n$ ($n = 1$ or 2) closely parallel those of the corresponding molybdenum(IV) system, $Mo(cp)Cl_3L_n$, in that no evidence for the formation of the more saturated $n = 2$ product is obtained for the bulkier $PMePh_2$ ligand, whereas both $n = 1$ and 2 systems can be obtained for both metals with PMe_3 and PMe_2Ph. For both niobium(IV) and molybdenum(IV) systems, the reaction between $M(cp)Cl_3(PMe_3)$ and PMe_3 proceeds too far for accurate equilibrium measurements. With PMe_2Ph, on the other hand, a measurable equilibrium is established for the niobium(IV) system. While the equilibrium is sufficiently rapid for the niobium(IV) system, it is much slower for Mo^{IV}. The thermal decomposition of the molybdenum(IV) complexes at elevated temperature prevented determination of the thermodynamic parameters experimentally for this system. The different rates of the two metal systems could be related to the spin change which is present for the molybdenum(IV) equilibrium [triplet for the 16-electron monophosphine complex, singlet for the 18-electron bis(phosphine) complex] but absent for the niobium(IV) equilibrium (doublet for both 15- and 17-electron complexes). While a spin-forbiddance factor is probably not important for organometallic reactions, an extra spin-change-related barrier could be introduced by the necessary structural rearrangement to achieve the spin crossover point, as we have shown for the addition of N_2 to $Mo(\eta\text{-}C_5Me_5)Cl(PMe_3)_2$.[5]

The experimental and theoretical investigations converge to the establishment of several facts. First, the addition of L (PMe_2Ph in the experimental work, PH_3 in the theoretical calculations) to $M(cp)Cl_3L$ is thermodynamically favored for both M = Nb and Mo. The measured enthalpy for the PMe_2Ph addition to **2** is -19.0 ± 1.6 kcal mol^{-1}. Since all participants to the equilibrium are solids (the niobium complexes) or liquids (PMe_2Ph), this value also approximately corresponds to the ΔE of the reaction [*i.e.* the Nb–PMe_2Ph bond dissociation energy (BDE) is 19.6 ± 1.6 kcal mol^{-1}]. By comparison, the calculated value for the Nb–PH_3 BDE is 21.3 kcal mol^{-1}. The agreement between the experimental Nb–PMe_2Ph BDE and the calculated Nb–PH_3 BDE is fortuitous and most likely arises from the choice of PH_3 as a model. Since PH_3 has a BDE which is intrinsically lower than the BDE of PR_3 and the MP2 computations usually overestimate BDEs, there is probably a cancellation of errors.[31] In addition, there may be basis set superposition error effects given that the basis set used is not very large.

The enthalpy for the PMe_2Ph addition to compound **7** could not be accurately measured because of the slow equilibrium at room temperature and thermal decomposition at higher temperature (see Results section). The calculated Mo–PH_3 BDE [relative to the $^3A''$ ground state of the 16-electron $Mo(cp)Cl_3(PH_3)$ system] is 23.5 kcal mol^{-1}. It is to be remarked that the MP2 calculations are based on a perturbative treatment of the electronic correlation, which is different in the two spin states. Consequently, although the BDEs obtained by the MP2 method will be more accurate than those available at the HF level, the calculation of the Mo–PH_3 BDE is subject to a greater error than that of the Nb–PH_3 BDE because of the spin state change. The calculated BDE relative to the excited $^1A'$ state (32.8 kcal mol^{-1}), on the other hand, is not subject to this error. Thus, this intrinsically stronger Mo–PH_3 interaction relative to the Nb–PH_3 interaction in the same oxidation state and ligand environment (by 11.5 kcal mol^{-1}) should be considered significant.

A second point of agreement between theory and experiment is the triplet ground state for the 16-electron $Mo(cp)Cl_3L$ system. Theoretically, the gap between ground state and excited singlet state is calculated as 9.3 kcal mol^{-1} for $L = PH_3$, which would place it in the IR region (3300 cm^{-1}). As stated above, a different calculation error may occur for the two different spin states because of the different extent of electronic correlation. Since the MP2 method is known to overestimate the effect of correlation, the energy of the more correlated system (*e.g.* the singlet) is likely to be artificially lowered to a greater extent by the perturbation Hamiltonian relative to that of the triplet state (*i.e.* the true singlet–triplet gap is likely to be greater than the calculated gap). Experimentally, this energy gap could not be measured. The $^3A'' \longrightarrow {}^1A'$ transition is spin forbidden and should therefore lead to a weak absorption.

Finally, with few exceptions, changes in the calculated geometric parameters on going from $Mo(cp)Cl_3L$ to $Mo(cp)Cl_3L_2$ or on going from $Nb(cp)Cl_3L_2$ to $Mo(cp)Cl_3L_2$ parallel the changes that are experimentally observed. Wherever a

Table 4 Selected atomic charges according to a natural population analysis on MP2-optimized $M(cp)Cl_3(PH_3)_n$ (M = Nb or Mo, n = 1 or 2)

	$Nb(cp)Cl_3(PH_3)$ ($S = \frac{1}{2}$)	$Nb(cp)Cl_3(PH_3)_2$ ($S = \frac{1}{2}$)	$Mo(cp)Cl_3(PH_3)$ ($S = 1$)	$Mo(cp)Cl_3(PH_3)$ ($S = 0$)	$Mo(cp)Cl_3(PH_3)_2$ ($S = 0$)
M	0.964	0.595	0.746	0.570	0.149
C, average	−0.2584	−0.2472	−0.2282	−0.2105	−0.2014
Cl, average	−0.459	−0.493	−0.464	−0.446	−0.485
P	0.226	0.271	0.286	0.318	0.371
H (PH_3), average	0.0396	0.0404	0.0438	0.0390	0.0354

discrepancy is observed, this discrepancy is rather small and could result from the different nature of the ligands in the two structurally characterized examples. For instance, the Mo–P distance appears to be more sensitive to the phosphine steric bulk than to the electronic configuration [*cf.* compounds $Mo(\eta\text{-}C_5Me_5)Cl_3(PMe_3)$, $Mo(\eta\text{-}C_5Me_5)Cl_3(PMePh_2)$ and $Mo(cp)Cl_3(PMe_2Ph)_2$ in Table 3].

The goal of this work was the estimation of how much the spin state change facilitates the dissociation of L on going from the diamagnetic $Mo(cp)Cl_3L_2$ to the paramagnetic ($S = 1$) $Mo(cp)Cl_3L$. According to the calculations for $L = PH_3$ (see Fig. 3), this figure amounts to almost 10 kcal mol^{-1}. At the outset of these investigations we expected to find a smaller Mo^{IV}–L BDE relative to the Nb^{IV}–L BDE, indeed because of the thermodynamic help of this spin change. However, both experimental and theoretical evidence point to the opposite trend of bond dissociation energies. We must therefore find reasons for the M–L bond to be intrinsically stronger for Mo^{IV} relative to Nb^{IV}.

The optimized geometric parameters give some indication as to the nature of this phenomenon. To the best of our knowledge, no discussion of the variation of M–Cl and $M–PR_3$ bond lengths on going from Nb to Mo is available in the literature, either on the basis of experimental data or on the basis of values optimized by computational methods. The available experimental data are abundant for M–Cl parameters, but rather limited for $M–PR_3$ parameters,[32] while theoretical computations focusing on these particular bonding parameters have not been previously available. To a first approximation, all bonds lengths should decrease on going from Nb to Mo because of the decrease in covalent radius. For the M–Cl distances, a small shortening is indeed observed for $M(cp)Cl_3(PH_3)$ (<0.03 Å) and no substantial difference is seen for $M(cp)Cl_3(PH_3)_2$ (*cf.* Tables 2 and 3). Conversely, the M–P bond length shows a much larger difference, the Nb–P bond length being 0.1 to 0.2 Å longer than the Mo–P bond length for both 15/16-electron and 17/18-electron Nb/Mo complexes. The average M–cp distance also shortens on going from Nb to Mo (>0.1 Å for the more saturated system, *ca.* 0.05 Å for the less saturated one). Obviously, there must be effects at play in addition to the change of covalent radius.

A first possible explanation is back bonding to the phosphine and cp ligands. Since Nb^{IV} and Mo^{IV} have d^1 and d^2 electronic configurations, respectively, there is one more electron in the molybdenum system which can be involved in back bonding to the ligands. Analogously, we could expect that the potentially π-donor Cl atoms are better capable of reinforcing the M–Cl bonds for the electronically poorer niobium(IV) center. In this case, the large contraction of M–P and M–cp distances on going from Nb to Mo could be solely or mostly attributed to the decrease of atomic radius, while the almost equivalent M–Cl distances would result from the compensation of two opposite effects: a decrease of metal radius and a decrease of M–Cl π bonding. Obviously, both effects may be operational at the same time.

The presence of M–Cl π bonding seems to be demonstrated by the experimental lengthening, rather than shortening, of this distance on going from Nb to Mo for a large collection of complexes.[32] A closer look at Tables 2 and 3 further supports this view: as mentioned in the Results section, the metal electrons in the $M(cp)Cl_3L_2$ complexes participate in M–Cl π bonding with the equatorial Cl ligands but not with the axial one [Scheme 2(*b*)]. Therefore, the axial M–Cl bond is not perturbed by the occupation of the d_{xy} orbital. The Tables show that this distance slightly shortens (by 0.008 Å) on going from Nb to Mo in agreement with the expected atomic radius contraction. On the other hand, the equatorial M–Cl bonds correspondingly lengthen by 0.020 Å. If we take the 0.008 Å shortening of the axial Mo–Cl distance as a basis for the atomic radius contraction on going from Nb to Mo, then the deviations from this value observed for the variations in the M–P and M–cp distances may be attributed to changes in M–P π and M–cp δ interactions.

The presence of back bonding to the phosphine and cp ligands does not have sufficient experimental back-up for lack of comparable niobium and molybdenum crystal structures. An additional computational result in favor of the presence of M–P π bonding comes from the analysis of the P–H distances. For the calculations reported here, only the P–H σ* orbitals of free PH_3 can serve as the phosphine π-acceptor orbitals, since phosphorus d-polarization functions were not included in the calculations. Previous theoretical work argues that these acceptor orbitals are sufficient to rationalize molecular changes attributable to M–P π back bonding.[33,34] There is also ample experimental evidence for the involvement of P–X σ* orbitals in M–P π back bonding in complexes of PX_3 ligands.[35,36] In essence, it has been found that a greater extent of M–P π bonding populates P–X σ* orbitals and therefore weakens the P–X interaction. For our geometry-optimized complexes of Nb^{IV} and Mo^{IV}, we find that the average P–H distance is slightly longer, although by a very small amount, for the 18-electron $Mo(cp)Cl_3(PH_3)_2$ relative to the 17-electron $Nb(cp)Cl_3(PH_3)_2$, as well as for the 16-electron ($S = 0$) $Mo(cp)Cl_3Mo(PH_3)$ relative to the 15-electron $Nb(cp)Cl_3Mo(PH_3)$ (*cf.* Tables 2 and 3). It is interesting that the average P–H distance also lengthens on going from $M(cp)Cl_3(PH_3)$ to $M(cp)Cl_3(PH_3)_2$ for both M = Nb (15- to 17-electron, Table 2) and Mo (16- to 18-electron, Table 3). This would suggest that the additional electron density donated by the second PH_3 ligand increases the π donation to each individual ligand, even though there is now one additional π acid competing for this electron density.

Additional interesting information is provided by a natural population analysis,[37] which provides the effective atomic charges shown in Table 4. The greatest variations are observed for the phosphorus charges. These variations indicate stronger M–P σ bonding for Mo relative to Nb. On going from Nb to Mo, the phosphorus charge increases by 0.060 (triplet) and 0.092 (singlet) in the mono-PH_3 series, and by 0.100 in the bis-PH_3 series. A stronger Mo–P σ bond finds a rationale in the better atomic energy match, since the molybdenum d electrons are less screened from the nuclear charge than is the niobium d electron. The greater effective charge on P should correspondingly induce a greater effective charge on the PH_3 hydrogen atoms. On the other hand, the observed variations of charge on H are often in the opposite direction (see Table 4). This can be attributed to the superposition of the σ and π effects. Indeed, the increase of π back donation into the P–H σ* orbitals on going from Nb to Mo ought to increase the population of the H

atom 1s orbitals and reduce the effective positive charge on these atoms. A reduction of positive charge of H, for instance, is observed on going from the 17-electron niobium, or from the 16-electron molybdenum complex (in either spin state) to the 18-electron molybdenum complex. In conclusion, the combined changes of effective charges on P and H are consistent with an increase of both σ and π components of the M–PH_3 bond on going from Nb to Mo.

Other trends that are evident from Table 4 are the expected decrease of metal charge upon co-ordination of PH_3, or upon going from Nb to Mo, or upon going from the 16-electron triplet molybdenum complex to the corresponding singlet complex. The variations in effective charge of Cl are also as expected. In particular co-ordination of PH_3 forces the Cl ligands to donate less to the metal. The decrease of effective negative charge on the cp carbon atoms on going from Nb to Mo parallels the increase of positive charge on the P atoms and indicates greater donation to the Mo.

A curious and currently unclear result of the natural population analysis is the increase of effective charge on the P atoms, and the corresponding decrease of negative charge on the cyclopentadienyl C atoms, on going from the mono- to the bis-PH_3 complex for each metal system, indicating that the PH_3 and cp ligands counterintuitively engage in stronger σ (for PH_3) or σ + 2π (for cp) interactions with the electron-richer metal center. This phenomenon will be the subject of further investigations. Thus, the observed shortening of the M–P bond upon co-ordination of PH_3 would result from the strengthening of *both* σ and π components of the M–P bond.

A difference in the extent of the M–Cl bond reorganization upon going from the mono- to the bis-phosphine derivative for each metal system affects in principle the thermodynamic strength of the M–PH_3 bond. The M–Cl distances lengthen by *ca.* 0.1 Å upon co-ordination of PH_3, in accord with the expected partial disruption of M–Cl π bonding and the decrease of effective positive charge on the metal. However, the extent of this bond lengthening is about the same for the two metal systems, indicating that the M–Cl bond reorganization is probably not the main cause for the difference in M–P bond strength. It seems thus more probable that the cause for the stronger Mo–PH_3 relative to the Nb–PH_3 bond has to be sought in the M–P interaction itself. The main difference between the Nb–P and the Mo–P bonds is that the latter shows evidence (see above) for a greater extent of both σ bonding and π back bonding.

Conclusion

The M(cp)Cl_3(PMe_2Ph)$_2$ systems are in equilibrium with the corresponding M(cp)Cl_3(PMe_2Ph) and free PMe_2Ph for both M = Nb and Mo. Only for M = Nb this equilibrium is sufficiently rapid to allow an experimental determination of the M–PMe_2Ph binding energy. The computational work affords geometries and relative energies in reasonable accord with experiment wherever experimental data are available. A comparison between the niobium and molybdenum system indicates an intrinsically stronger Mo–PH_3 bond relative to Nb. This is attributed to a greater extent of both σ bonding and π back bonding for the d^2 metal center. The effective bond strength, however, is comparable for the two metals as a result of the regain of pairing energy upon adoption of a spin triplet ground state for the less saturated molybdenum system.

Acknowledgements

We are grateful to the National Science Foundation (grant CHE-9508521) for support and to Professor Cary Miller for use of his DEC AlphaStation 250 at the University of Maryland, which was purchased with NSF grant CHE-9417357. We also thank Drs. Antonio Rizzo and Ivo Cacelli for helpful discussion.

References

1 R. Poli, *Acc. Chem. Res.*, in the press.
2 R. Poli, *Chem. Rev.*, 1996, **96**, 2135.
3 F. Calderazzo, G. Fachinetti and C. Floriani, *J. Am. Chem. Soc.*, 1974, **96**, 3695.
4 H. H. Brintzinger, L. L. Lohr, jun. and K. L. T. Wong, *J. Am. Chem. Soc.*, 1975, **97**, 5146.
5 D. W. Keogh and R. Poli, *J. Am. Chem. Soc.*, 1997, **119**, 2516.
6 R. Poli, B. E. Owens and R. G. Linck, *J. Am. Chem. Soc.*, 1992, **114**, 1302.
7 F. Abugideiri, J. C. Gordon, R. Poli, B. E. Owens-Waltermire and A. L. Rheingold, *Organometallics*, 1993, **12**, 1575.
8 J. Daran, K. Prout, A. de Cian, M. L. H. Green and N. Siganporia, *J. Organomet. Chem.*, 1977, **136**, C4.
9 M. J. Bunker and M. H. L. Green, *J. Chem. Soc., Dalton Trans.*, 1981, 85.
10 R. J. Burt, G. J. Leigh and D. L. Hughes, *J. Chem. Soc., Dalton Trans.*, 1981, 793.
11 J. C. Fettinger, D. W. Keogh and R. Poli, *Inorg. Chem.*, 1995, **34**, 2343.
12 A. M. Cardoso, R. J. H. Clark and S. Moorhouse, *J. Chem. Soc., Dalton Trans.*, 1980, 1156.
13 J. de la Mata, R. Fandos, M. Gomez, P. Gomez-Sal, S. Martinez-Carrera and P. Royo, *Organometallics*, 1990, **9**, 2846.
14 R. Poli, S. T. Krueger, F. Abugideiri, B. S. Haggerty and A. L. Rheingold, *Organometallics*, 1991, **10**, 3041.
15 K. Raner, CURVE FIT, version 0.7e, Clayton, Victoria, 1992.
16 M. J. Frisch, G. W. Trucks, H. B. Schlegel, P. M. W. Gill, B. G. Johnson, M. A. Robb, J. R. Cheeseman, T. A. Keith, G. A. Petersson, J. A. Montgomery, K. Raghavachari, M. A. Al-Laham, V. G. Zakrzewski, J. V. Ortiz, J. B. Foresman, J. Cioslowski, B. B. Stefanov, A. Nanayakkara, M. Challacombe, C. Y. Peng, P. Y. Ayala, W. Chen, M. W. Wong, J. L. Andres, E.S. Replogle, R. Gomperts, R. L. Martin, D. J. Fox, J. S. Binkley, D. J. Defrees, J. Baker, J. P. Stewart, M. Head-Gordon, C. Gonzales and J. A. Pople, GAUSSIAN 94 (Revision A1), Gaussian Inc., Pittsburgh, PA, 1995.
17 P. J. Hay and W. R. Wadt, *J. Chem. Phys.*, 1985, **82**, 299.
18 W. R. Wadt and P. J. Hay, *J. Chem. Phys.*, 1985, **82**, 284.
19 P. J. Hay and W. R. Wadt, *J. Chem. Phys.*, 1985, **82**, 270.
20 R. Poli and H. D. Mui, *Inorg. Chem.*, 1991, **30**, 65.
21 R. Poli and M. A. Kelland, *J. Organomet. Chem.*, 1991, **419**, 127.
22 A. A. Cole, J. C. Fettinger, D. W. Keogh and R. Poli, *Inorg. Chim. Acta*, 1995, **240**, 355.
23 A. Cole, J. C. Gordon, M. A. Kelland, R. Poli and A. L. Rheingold, *Organometallics*, 1992, **11**, 1754.
24 S. T. Krueger, R. Poli, A. L. Rheingold and D. L. Staley, *Inorg. Chem.*, 1989, **28**, 4599.
25 I. Cacelli, D. W. Keogh, R. Poli and A. Rizzo, unpublished work.
26 I. Cacelli, D. W. Keogh, R. Poli and A. Rizzo, *New J. Chem.*, 1997, **21**, 133.
27 K. Prout and J.-C. Daran, *Acta Crystallogr., Sect. B*, 1979, **35**, 2882.
28 R. Poli, *Organometallics*, 1990, **9**, 1892.
29 P. Kubácek, R. Hoffmann and Z. Havlas, *Organometallics*, 1982, **1**, 180.
30 Z. Lin and M. B. Hall, *Organometallics*, 1993, **12**, 19.
31 R. Schmid, W. A. Herrmann and G. Frenking, *Organometallics*, 1997, **16**, 701.
32 A. G. Orpen, L. Brammer, F. H. Allen, O. Kennard, D. G. Watson and R. Taylor, *J. Chem. Soc., Dalton Trans.*, 1989, S1.
33 D. S. Marynick, *J. Am. Chem. Soc.*, 1984, **106**, 4064.
34 J. A. Tossell, J. H. Moore and J. C. Giordan, *Inorg. Chem.*, 1985, **24**, 1100.
35 A. G. Orpen and N. G. Connelly, *Organometallics*, 1990, **9**, 1206.
36 A. G. Orpen and N. G. Connelly, *J. Chem. Soc., Chem. Commun.*, 1985, 1310.
37 E. D. Glendening, A. E. Reed, J. E. Carpenter and F. Weinhold, NBO, Version 3.1; A. E. Reed, L. A. Curtiss and F. Weinhold, *Chem. Rev.*, 1988, **88**, 899.

Received 6*th May* 1997; *Paper* 7/03070C